

Boost converter trajectory planning by exact tracking error dynamics passive output feedback (ETEDPOF)

Planificación de trayectorias del convertidor boost por realimentación de la salida pasiva de la dinámica exacta del error de seguimiento (ETEDPOF)

Sosa, Keiver^{1*}; Spinetti, Mario²; Colina-Morles, Eliezer³

1 Doctorado en Ciencias Aplicadas, Facultad de Ingeniería.

Universidad de Los Andes, Mérida, Venezuela,

2 Dpto. de Sistemas de Control, Escuela de Ing. de Sistemas, Facultad de Ingeniería.

Universidad de Los Andes, Mérida, Venezuela,

3 Illinois Applied Research Institute, University of

Illinois Urbana-Champaign, USA

*keiversosa@gmail.com

Abstract

This work shows the integration of the theoretical ETEDPOF control technique in the experimental implementation of a Boost power converter. This includes semiconductor losses in the Boost converter's dynamics, which are used to calculate the controller and plan trajectories to monitor the output. The work includes simulations that facilitate a comparative analysis between the model and the laboratory results, which allows the validation of the methodology used.

Keywords: Non-linear Systems, Planned Trajectory, Boost Converter, ETEDPOF.

Resumen

Este trabajo muestra la integración de la técnica teórica de control ETEDPOF en la implementación experimental de un convertidor de potencia de refuerzo. Esto incluye pérdidas de semiconductores en la dinámica del convertidor Boost, que se utilizan para calcular el controlador y planificar trayectorias para monitorear la salida. El trabajo incluye simulaciones que facilitan un análisis comparativo entre el modelo y los resultados de laboratorio, lo que permite la validación de la metodología utilizada.

Palabras clave: Sistemas No Lineales, Planificación de Trayectorias, Convertidor Boost, ETEDPOF.

1 Introduction

In this paper, we want to bring mathematical concepts closer to the experimental results obtained in the laboratory. The Boost converter dynamic model does not consider the devices' losses in the experimental implementation. The Joule dynamic model of the Boost converter is used to improve the dynamic model of the converter; this includes some of the losses due to the conductors and semiconductors of the circuit assembled in the laboratory. Using the Joule model, the Exact

Tracking Error Dynamics Passive Output Feedback (ETEDPOF) control technique is applied, which has the property to track trajectories. A trajectory to bring the output from an initial operating point to a final one, following a smooth tracking function, is planned. The technique leads to algorithms programmed to solve the control problem, trajectory planning, and the pulse width modulator design. Computer simulations of the continuous model, including the pulse width modulator (PWM) and the real-time implementation of the Boost converter trajectory planning, were implemented in the laboratory to validate the system's behavior.

2 Dynamics of Boost Converter Including Joule Model

The DC-DC Boost power converter is also known as the “up-converter” because it increases the output voltage concerning the power supply. This Converter is frequently used in much electrical and electronic equipment. Fig.1 shows a simplified electrical diagram. This model is called Boost Ideal Converter because it does not include the energy losses associated with the electrical and electronic devices of the power converter. An average model for this Converter, using the Kirchhoff and Ohm laws, may be obtained straightforwardly as:

$$\begin{aligned} L \frac{dx_1(t)}{dt} &= E - (1-u(t))x_2(t), \\ C \frac{dx_2(t)}{dt} &= (1-u(t))x_1(t) - \frac{x_2(t)}{R}, \end{aligned} \quad (1)$$

where the variable $x_1(t)$ represents the inductor current, $x_2(t)$ is the capacitor voltage or output voltage, and $u(t)$ is the control action. The parameters are L the inductance, C the capacitance, E the power supply and R the load resistor. The variables $x_1(t)$, $x_2(t)$, $u(t)$ are written as x_1 , x_2 , u for convenience.

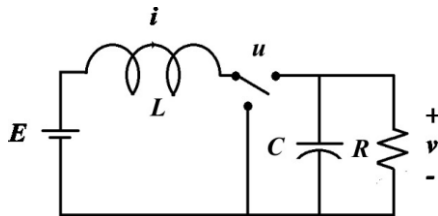


Fig. 1. Ideal Boost Converter.

When the simulations of the ideal Boost model are compared with the measurements made in the physical Boost implementation, we get a significant discrepancy. To improve the dynamic model, we include characteristics of the materials, such as resistance of the conductors, voltage drops of the semiconductors, and losses because of the current conduction, among others. These characteristics are taken from the semiconductor models presented by Millman (1979). All of these are energy losses converted into heat due to the converter current. For this reason, we will call the proposed model Joule Boost Converter, presented in Fig. 2; this model is referenced in Spinetti (2010).

The dynamic model of the Joule model of the Boost converter is obtained and represented in the matrix form equation (2)

$$\begin{aligned} \begin{bmatrix} L & 0 \\ 0 & C \end{bmatrix} \begin{bmatrix} \dot{x}_1 \\ \dot{x}_2 \end{bmatrix} &= \begin{bmatrix} 0 & -(1-u) \\ (1-u) & 0 \end{bmatrix} \begin{bmatrix} x_1 \\ x_2 \end{bmatrix} + \begin{bmatrix} E \\ 0 \end{bmatrix} \\ - \begin{bmatrix} R_{in} + R_j & 0 \\ 0 & \frac{1}{R} \end{bmatrix} \begin{bmatrix} x_1 \\ x_2 \end{bmatrix} &- \begin{bmatrix} V_q \\ 0 \end{bmatrix} u - \begin{bmatrix} V_f \\ 0 \end{bmatrix} (1-u), \end{aligned} \quad (2)$$

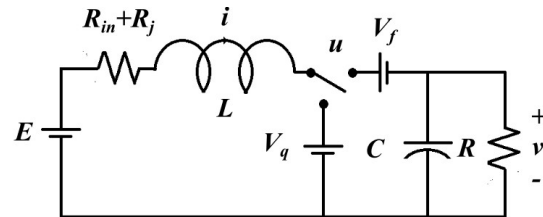


Fig. 2. Joule Boost Converter.

where R_{in} represents the internal inductor resistance, R_j represents the sum of the resistive losses distributed by the conductors, V_q is the voltage drop transistor in conduction, V_f is the diode in conduction voltage drop; this extended model refers to the losses due to the Joule effect. The parameter R_{in} is obtained directly by measuring the coil's internal resistance and the other parameters are approximated using the circuit's physical implementation. The voltages V_q and V_f are measured directly by the transistor and the diode in conduction. R_j is adjusted to approximate the most significant losses in the circuit.

2.1 Boost Joule Model Equilibria.

By setting the dynamics of equation (2) to zero, the equilibrium coordinates (\bar{x}_1, \bar{x}_2) are obtained in terms of the parameters of the Joule Boost model, for an equilibrium value of the input \bar{u} . For the purposes of the controller, a desired output voltage value $\bar{x}_2 = V_d$ is chosen and the pair (\bar{x}_1, \bar{u}) is solved. Then, the equilibria are (3).

$$\begin{aligned} \bar{x}_1 &= \frac{(E - V_q)}{2(R_{in} + R_j)} - \sqrt{\frac{(E - V_q)^2}{4(R_{in} + R_j)^2} - \frac{(V_f - V_q + \bar{x}_2)\bar{x}_2}{R(R_{in} + R_j)}}, \\ \bar{u} &= 1 - \frac{\bar{x}_2}{\bar{x}_1 R} \end{aligned} \quad (3)$$

where \bar{x}_1 is the steady state inductor current value, \bar{x}_2 is the steady state capacitor voltage value, and \bar{u} the steady state control value.

3 Controller Synthesis for Boost Joule Model.

The technique used to design the feedback controller for the Boost converter is called Exact Tracking Error Dynamics Passive Output Feedback (ETEDPOF). Some references to this technique can be found in Sira-Ramirez and Fliess (2004), Sira-Ramirez (2005), Sira-Ramirez and Silva-Ortigoza (2006) and Spinetti (2010). Specifically, Sira-Ramirez (2005) explains the technique in detail, and Spinetti (2010) includes examples that show how it is applied to power converters.

To apply the ETEDPOF technique, the exact dynamics of the tracking error, calculated as the difference between the original system and a reference dynamic system is needed. That is represented through the superscript * and is expressed through the following equation:

$$\begin{bmatrix} L & 0 \\ 0 & C \end{bmatrix} \begin{bmatrix} \dot{x}_1^* \\ \dot{x}_2^* \end{bmatrix} = \begin{bmatrix} 0 & -(1-u^*) \\ (1-u^*) & 0 \end{bmatrix} \begin{bmatrix} x_1^* \\ x_2^* \end{bmatrix} + \begin{bmatrix} E \\ 0 \end{bmatrix} \quad (4)$$

$$-\begin{bmatrix} R_m + R_j & 0 \\ 0 & 1/R \end{bmatrix} \begin{bmatrix} x_1^* \\ x_2^* \end{bmatrix} - \begin{bmatrix} V_q \\ 0 \end{bmatrix} u - \begin{bmatrix} V_f \\ 0 \end{bmatrix} (1-u^*)$$

The difference between (2) and (4) is that the first is disturbed and the second is not; it is also assumed that as $t \rightarrow \infty$ the error $e \rightarrow 0$. The steady state value of the reference system is the same, therefore, $\bar{x}_1^* = \bar{x}_1$, $\bar{x}_2^* = \bar{x}_2$ and $\bar{u}^* = \bar{u}$. The error dynamics are calculated through $e_1 = x_1 - \bar{x}_1^*$, $e_2 = x_2 - \bar{x}_2^*$ and $e_u = u - \bar{u}^*$, where e_1 is the inductor current error, e_2 is the capacitor voltage error, and e_u is the control error. Then the error dynamics takes the form (5).

$$\begin{bmatrix} L & 0 \\ 0 & C \end{bmatrix} \begin{bmatrix} \dot{e}_1 \\ \dot{e}_2 \end{bmatrix} = \begin{bmatrix} 0 & -(1-u) \\ (1-u) & 0 \end{bmatrix} \begin{bmatrix} e_1 \\ e_2 \end{bmatrix} \quad (5)$$

$$-\begin{bmatrix} R_m + R_j & 0 \\ 0 & 1/R \end{bmatrix} \begin{bmatrix} e_1 \\ e_2 \end{bmatrix} + \begin{bmatrix} V_f - V_q + \bar{x}_2^* \\ -x_1^* \end{bmatrix} e_u$$

Using the auxiliary variable $e_u = -\gamma e_y$ where γ is a positive constant, the passive output is defined by the equation (6),

$$e_y = B^{*T} e = \begin{bmatrix} V_f - V_q + \bar{x}_2^* & -x_1^* \end{bmatrix} \begin{bmatrix} e_1 \\ e_2 \end{bmatrix} \quad (6)$$

$$e_y = (V_f - V_q + \bar{x}_2^*)e_1 - x_1^*e_2$$

Now, using the passive output it's possible to synthe-

size the controller by ETEDPOF, which is shown in the equation (7),

$$u = u^* - \gamma \left((V_f - V_q + \bar{x}_2^*)e_1 - x_1^*e_2 \right) \quad (7)$$

$$u = u^* - \gamma \left((V_f - V_q)(x_1 - x_1^*) + \bar{x}_2^*x_1 - x_1^*x_2 \right)$$

To guarantee convergence to equilibrium, that is, when $t \rightarrow \infty$ the error system $e \rightarrow 0$, it is necessary to demonstrate that the closed-loop system is stable.

4 Stability Analysis.

The stability analysis is performed using the Lyapunov method, for which a candidate function $V(e)$ that is positive definite is used. Therefore $V(e) = \frac{1}{2} e^T A e > 0$, where

e is the state vector of the error dynamics, $e^T = [e_1 \ e_2]$ and $A = \begin{bmatrix} L & 0 \\ 0 & C \end{bmatrix}$ is the matrix of converter constants. Fur-

thermore, it must be true that $V(0) = 0$ and $e(t) \neq 0$.

Then the quadratic candidate function becomes

$$V(e) = \frac{1}{2} \begin{bmatrix} e_1 \\ e_2 \end{bmatrix}^T \begin{bmatrix} L & 0 \\ 0 & C \end{bmatrix} \begin{bmatrix} e_1 \\ e_2 \end{bmatrix} > 0. \quad (8)$$

Using the Lyapunov Theorem if $\dot{V}(e) < 0$ then $e \rightarrow 0$, in other words, the system is stable. The derivative

of (8) $\dot{V}(e) = \begin{bmatrix} e_1 \\ e_2 \end{bmatrix}^T \begin{bmatrix} L & 0 \\ 0 & C \end{bmatrix} \begin{bmatrix} \dot{e}_1 \\ \dot{e}_2 \end{bmatrix}$ using the equation (5) in the last equation is obtained

$$\dot{V}(e) = e^T \begin{bmatrix} 0 & -(1-u) \\ (1-u) & 0 \end{bmatrix} e - e^T \begin{bmatrix} R_m + R_j & 0 \\ 0 & 1/R \end{bmatrix} e \quad (9)$$

$$- \gamma e^T \begin{bmatrix} V_f - V_q + \bar{x}_2^* \\ -x_1^* \end{bmatrix} \begin{bmatrix} V_f - V_q + \bar{x}_2^* \\ -x_1^* \end{bmatrix}^T e.$$

The antisymmetric term of the equation (9) cancels, so to ensure stability it is enough to show that the equation (10) is true, since this implies that $\dot{V}(e) < 0$ and that system is Lyapunov stable.

$$\begin{bmatrix} \frac{(R_m + R_j)}{\gamma} + (V_f - V_q + \bar{x}_2^*)^2 & -\bar{x}_1^* (V_f - V_q + \bar{x}_2^*) \\ -\bar{x}_1^* (V_f - V_q + \bar{x}_2^*) & \frac{1}{\gamma R} + \bar{x}_1^{*2} \end{bmatrix} > 0. \quad (10)$$

The matrix of the equation (10) is positive definite if the following conditions are true, according to Sylvester's criterion (García and Maza, 2013)

$$g(V_f - V_q + x_2^*)^2 + \frac{R_{in} + R_j}{\gamma} > 0,$$

$$g \frac{R_{in} + R_j}{\gamma} + R(R_{in} + R_j)x_1^{*2} + (V_f - V_q + x_2^*)^2 > 0.$$

Both conditions are true because all resistance are positive and $\gamma > 0$.

5 Trajectory Planning.

A SISO system is said to be *flat* if there exists an endogenous variable, called the flat output, denoted by f , such that the input u and the output y can in turn be expressed as a linear combination of the flat output and a finite number of its time derivatives, i.e., that y and u are differential functions of the flat output f (Sira-Ramirez and Agrawal (2004)).

The Boost Converter is a differentially flat dynamic system with respect to its energy (F) ((Sira-Ramirez and Agrawal (2004)). We will use F as a function to obtain a planned trajectory.

The power in the ideal inductor and capacitor are given by $P_L = Lx_1\dot{x}_1$ and by $P_C = Cx_2\dot{x}_2$, therefore the energy stored in the converter is $F = Lx_1^2 + Cx_2^2$. In this case, the Boost Joule model has a certain variation due to the losses inherent to the elements; however, an equation proportional to the energy equation of the ideal model is used as a planning function, expressed by

$$F^* = \frac{1}{2}Lx_1^{*2} + \frac{1}{2}Cx_2^{*2} \quad (11)$$

and deriving (11) is obtained (12)

$$\dot{F}^* = x_1^*E - (R_{in} + R_j)x_1^{*2} - x_1^*V_f - x_1^*u^*(V_q - V_f) - \frac{x_2^{*2}}{R}. \quad (12)$$

To use (12) the semiconductor voltages $V_q \approx V_f$ are approximated to eliminate the dependence of the control, then the approximation that remains is the equation (13).

$$\dot{F}^* \approx (E - V_f)x_1^* - (R_{in} + R_j)x_1^{*2} - \frac{x_2^{*2}}{R} \quad (13)$$

This allows the output to be obtained as a function of the derivative of the energy:

$$x_2^{*2} = \left((E - V_f)x_1^* - (R_{in} + R_j)x_1^{*2} - \dot{F}^* \right) R \quad (14)$$

With the equations (13) and (14) the quadratic equation of the inductor current given by

$$x_1^{*2} + x_1^* \frac{(E - V_f)}{\left(\frac{L}{CR} - R \right)} - \frac{\dot{F}^* + \frac{2F^*}{CR}}{\left(\frac{L}{CR} - (R_{in} + R_j) \right)} = 0 \quad (15)$$

where the solutions are (16)

$$x_1^* = -\frac{(E - V_f)}{2\left(\frac{L}{CR} - (R_{in} + R_j) \right)} \pm \sqrt{\frac{1}{4\left(\frac{L}{CR} - (R_{in} + R_j) \right)^2} + \frac{\dot{F}^* + \frac{2F^*}{CR}}{\left(\frac{L}{CR} - (R_{in} + R_j) \right)}} \quad (16)$$

The equation (16) is derived obtaining

$$\dot{x}_1^* = \frac{\frac{\dot{F}^* + \frac{2F^*}{CR}}{\left(\frac{L}{CR} - (R_{in} + R_j) \right)}}{2\sqrt{\frac{1}{4\left(\frac{L}{CR} - (R_{in} + R_j) \right)^2} + \frac{\dot{F}^* + \frac{2F^*}{CR}}{\left(\frac{L}{CR} - (R_{in} + R_j) \right)}}} \quad (17)$$

Then the control to plan the trajectory is

$$u^* = \frac{L\dot{x}_1^* - E + R_{in}x_1^* + V_f + x_2^{*2}}{x_2^*} \quad (18)$$

5.1 Arbitrary Trajectory.

For planning, an arbitrary trajectory obtained through a Bezier polynomial is used. This has been reduced to three terms due to limitations of the processor, expressed by the equation (19),

$$\psi(\tau) = \begin{cases} 0 & t < t_i \\ \tau^5 (r_1 - r_2\tau + r_3\tau^2) & t_i < t < t_f \\ 1 & t > t_f \end{cases} \quad (19)$$

where $\tau = \frac{t - t_i}{t_f - t_i}$ and $r_1 = 21, r_2 = 35, r_3 = 15$.

For the reference system, both the energy function

(F^*) and its derivatives (\dot{F}^*, \ddot{F}^*) are required, so it is necessary that the reference signal used be, at least, continuous and differentiable up to the second order. For this, the reference trajectory of the energy function is selected, according to the equation (20),

$$F^* = \begin{cases} F_i^* & t < t_i \\ F_i^* + (F_f^* - F_i^*)\psi(t, t_i, t_f) & t_i < t < t_f \\ F_f^* & t > t_f \end{cases} \quad (20)$$

where F_i^* is the initial energy, F_f^* is the final energy and $\psi(t, t_i, t_f)$ is in this case a polynomial in $t \in [t_i, t_f]$ and that satisfies the conditions $\psi(t_i) = 0$, $\psi(t_f) = 1$, $\dot{\psi}(t_i) = \dot{\psi}(t_f) = \ddot{\psi}(t_i) = \ddot{\psi}(t_f) = 0$.

6 Simulations.

The converter parameters used are the following: $E = 10V$, $L = 33mH$, $C = 1000\mu F$, $R = 2\Omega$. The model parameters obtained from the measurements are $R_{in} = 0.05\Omega$, $R_j = 0.006\Omega$, $V_q = 1.05V$, $V_f = 1.14V$ and the controller gain $\gamma = 0.00001$.

The planned trajectory is to go from an initial condition (6A, 10V) to a final condition (26A, 20V) and change is through a smooth curve. The time is specified so that

- Remain $\Delta_{t_1} = 10$ msec in the initial condition.
- Follow the planned trajectory for $\Delta_{t_2} = 30$ msec.
- Remain $\Delta_{t_3} = 10$ msec in the final condition

In the Fig. 4 shows the inductor current (x_1^*), the capacitor voltage x_2^* and the signal Control u^* , the voltage includes the three time regions expressed in the equation (17), which includes two time periods making regulation Δ_{t_1} and Δ_{t_3} of 10 msecs and a period of time where a polynomial tracks the trajectory Δ_{t_2} . It should be noted that this simulation is for continuous control since the pulse width modulator (PWM) has not been included.

In other hand, Fig. 5 shows the energy function (F^*) used to track the planned trajectory and also includes the first and second derivative (\dot{F}^* , \ddot{F}^*), where it's observed that the three functions are smooth.

7 Experimental Implementation.

An experimental implementation of the Boost converter was set up to measure current in the inductor and voltage

in the capacitor. The circuit diagram is shown in the Fig. 3.

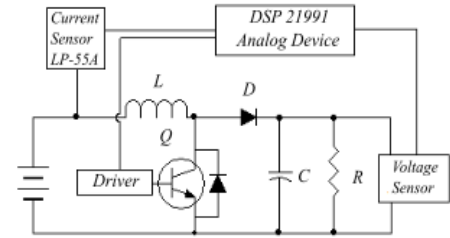


Fig. 3. Circuit Diagram Boost Converter.

The electronic device used is a IGBT, brand Siemens and model BSM200GB170DLC that acts as a transistor and diode. The feedback controller of the passive output is solved by means of an algorithm in the AD21991 digital signal processor (DSP).

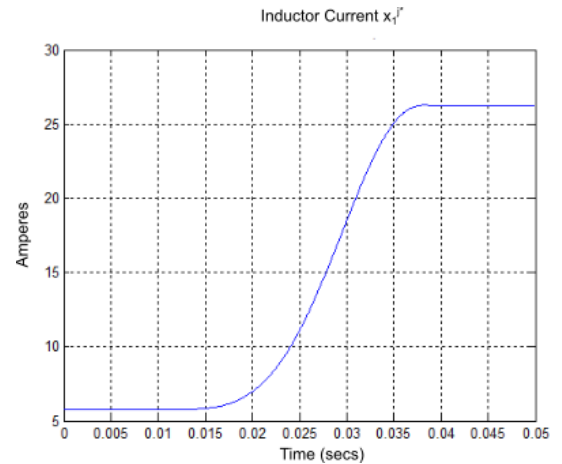


Fig. 4a. Inductor Current x_1^*

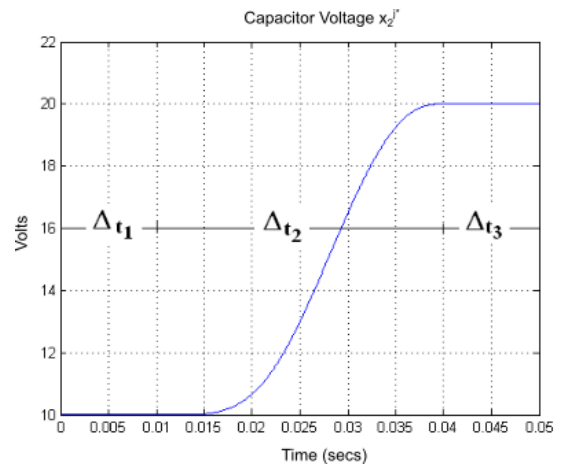


Fig. 4b. Capacitor Voltage x_2^*

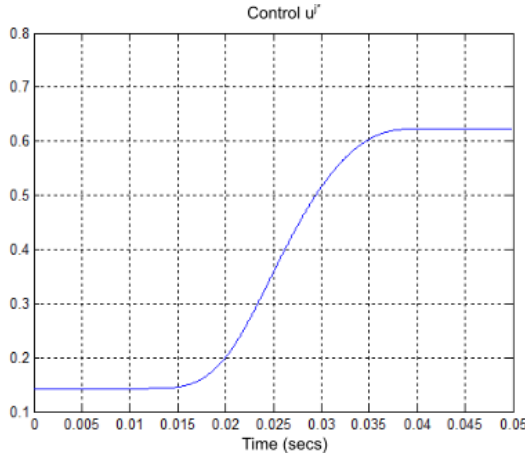


Fig. 4c. Control u^*

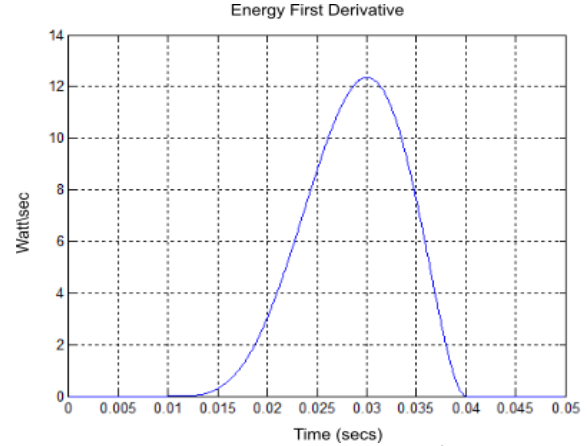


Fig. 5b. First Derivative of Energy \dot{F}^{j*}

Fig. 4. Simulations of Planned Trajectory $\psi(t, t_i, t_f)$ Variables

The implementation of the converter was done through an algorithm that includes the controller, the path planning function and the pulse width modulator (PWM). This algorithm is applied in the simulation and the experimental set-up. For this, we include three examples:

- Range from 13 to 17 volts the Fig. 6a and 6b corresponding to inductor current and capacitor voltage.
- Range from 14 to 16 volts the Fig. 7a and 7b corresponding to inductor current and capacitor voltage.

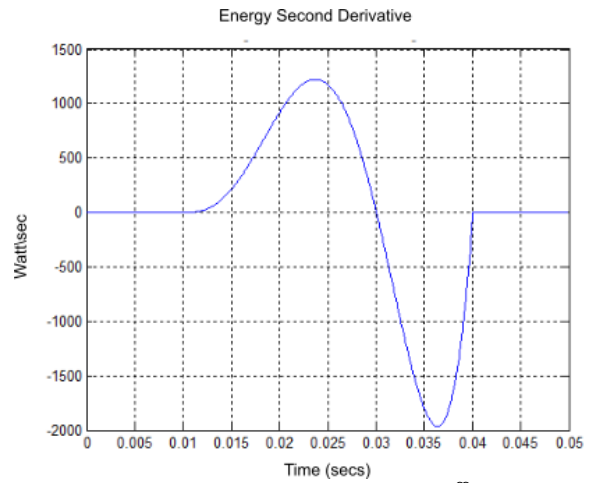


Fig. 5c. Second Derivative of Energy \ddot{F}^{j*}

Fig. 5. Simulations of Energy Function (F^{j*}) and its Derivatives (\dot{F}^{j*} , \ddot{F}^{j*}).

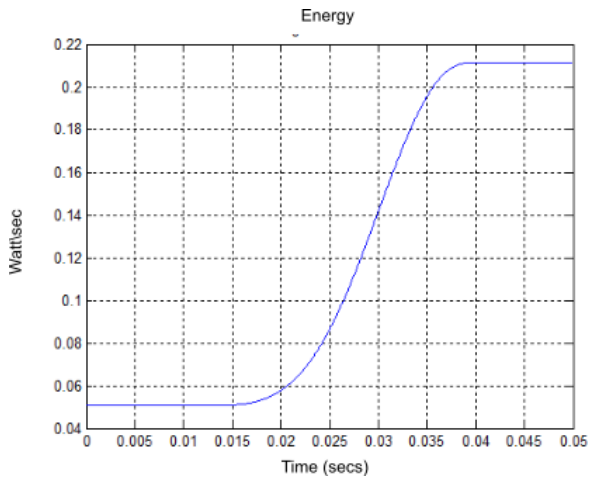


Fig. 5a. Energy Function F^{j*}

8 Analysis of Results.

The simulations and experimental results show agreement and the error committed in the monitoring is negligible, which corroborates the performance of the proposed control.

As can be seen the overall operation of the Joule model, the ETEDPOF controller, shows how they can sweep a large part of the operating range, namely $(E, 2E)$.

In general, it's shown that the entire operating range is covered by the behavior of the converter, in a precise way.

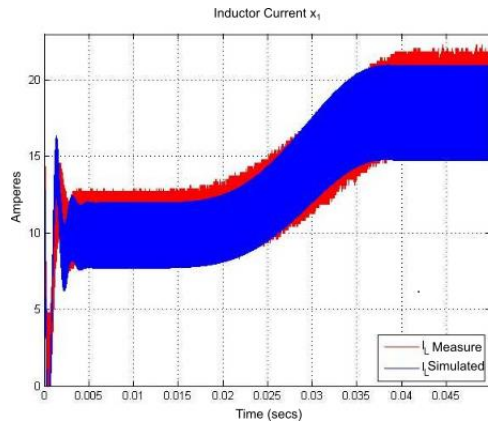


Fig. 6a. Inductor Current.

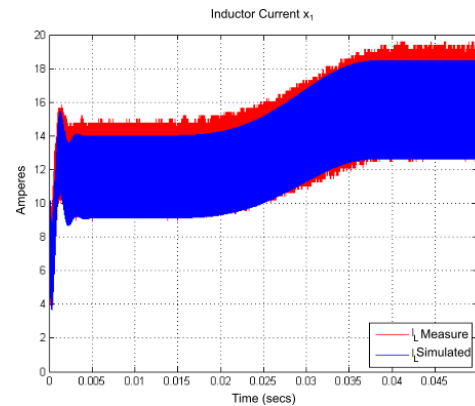


Fig. 7a. Inductor Current.

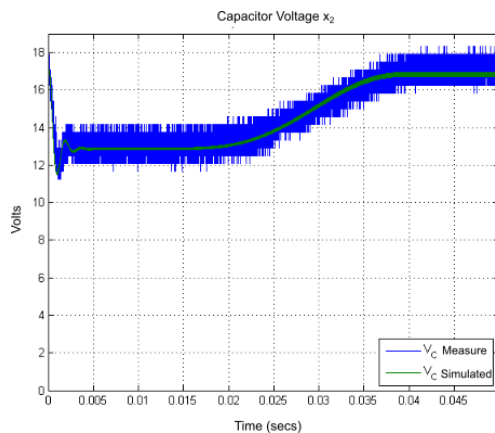


Fig. 6b. Capacitor Voltage.

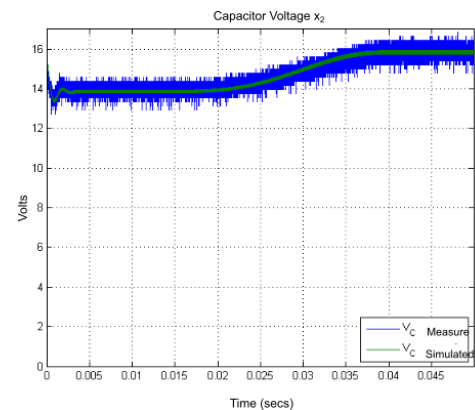


Fig. 7b. Capacitor Voltage.

Fig. 6. Simulations and Measurement Comparison.
Range 13-17 Volts.

Fig. 7. Simulations and Measurement Comparison.
Range 14-16 Volts.

In all cases, the measured signals use a periodic algorithm that repeats them cyclically, these forces initial conditions to be set before beginning each cycle, this is the reason why there's a small transient in the signals shown. These conditions are included in the simulations.

9 Conclusions.

- A dynamic model called the Joule model is shown, which better approximates the dynamics of the Boost converter behavior, including the losses of the conductors and semiconductors.
- The results of the ETEDPOF technique are functional in Boost converter and can be applied to others power converters.
- The Joule Model considers the ETEDPOF technique and the power losses due to the Joule effect.
- The proposed feedback control design technique produces a robust power converter response to variations and allows trajectory tracking.

References

- García, I. A. and Maza, S. (2013). Curso de Introducción al Cálculo para Grados en Ingeniería. Eines. Universitat de Lleida, ISBN 978-84-8409-603-0.
- Millman, J. (1979). *Micro-electronics; digital and analog circuits and systems: (M. Hill, Ed.)*.
- Sira-Ramirez, H. (2005). Are nonlinear controllers really necessary in power electronics devices? In European-conference in power electronics and applications(10pp.-P.10).Dresden,Germany.doi: 10.1109/EPE.2005.219747
- Sira-Ramirez, H., & Agrawal, S. (2004). *Differentially flat systems*. CRC Press. (ISBN 1315214652)
- Sira-Ramirez, H., & Fliess, M. (2004). *On the output feedback control of a synchronous generator*. In 43rd IEEE conference on decision and control (cdc) (IEEE Cat. No.04ch37601) (Vol. 4, p. 4459-4464). Nassau, Bahamas: IEEE. doi: 10.1109/CDC.2004.1429453
- Sira-Ramirez, H., & Silva-Ortigoza, R. (2006). *Control design techniques in power electronics devices*. Springer Science & Business Media.
- Spinetti, M. (2010). Síntesis de controladores para convertidores de potencia utilizando realimentación de la salida

pasiva de la dinámica exacta del error de seguimiento: teoría y práctica (Ph.D. dissertation). Universidad Politécnica de Cataluña, Barcelona, España.

Recibido: 10 abril 3 de 2024

Aceptado: 13 de agosto de 2024

Sosa, Keiver: Ingeniero de Sistemas y profesor agregado en la Universidad de Los Andes. Estudiante de doctorado en Ciencias Aplicadas e investiga en el área de sistemas de control, convertidores de potencia no lineales y aplicaciones prácticas. 3

 <https://orcid.org/0000-0002-3194-7059>

Spinetti, Mario: Ingeniero eléctrico, Doctor en Automatización Avanzada y Robótica. Profesor titular en la Universidad de Los Andes. Autor de artículos en el área de sistemas de control y convertidores de potencia no lineales. Correo electrónico: spinettimarios@gmail.com

 <https://orcid.org/0000-0002-2464-421X>

Colina-Morles, Eliezer: Systems Engineer at the University of Los Andes, M.D. in Systems Engineering from Case Western Reserve University Ph.D. in Intelligent Control Systems, from the University of Sheffield. Senior Research Engineer in Illinois Applied Research Institute, University of Illinois. Correo electrónico: ecolinamorles@gmail.com

 <https://orcid.org/0000-0003-0232-1003>